J. Cell. Mol. Med. Vol 14, No 1-2, 2010 pp. 242-256

PPARγ2 expression in growth plate chondrocytes is regulated by p38 and GSK-3

Lee-Anne Stanton, Jennifer Ruizhe Li, Frank Beier *

CIHR Group in Skeletal Development and Remodelling, Department of Physiology and Pharmacology, University of Western Ontario, London, Ontario, Canada

Received: March 14, 2008; Accepted: May 15, 2008

Abstract

Although peroxisome proliferator activated receptor (PPAR)γ remains a critical regulator of preadipocyte differentiation, new roles have been discovered in inflammation, bone morphogenesis, endothelial function, cancer, longevity and atherosclerosis. Despite the demonstration of PPARγ expression in chondrocytes, its role and the pathways affecting its expression and activity in chondrocytes remain largely unknown. We investigated the effects of PPARγ activation on chondrocyte differentiation and its participation in chondrocyte lipid metabolism. PPARγ2 expression is highly regulated during chondrocyte differentiation *in vivo* and *in vitro* PPARγ activation with troglitazone resulted in increased *Indian hedgehog* expression and reduced *collagen X* expression, confirming previously described roles in the inhibition of differentiation. However, the major effect of PPARγ2 in chondrocytes appears to be on lipid metabolism. During differentiation chondrocytes increase expression of the lipid-associated metabolizing protein, *Lpl*, which is accompanied by increased gene expression of *PPARγ*. *PPARγ* expression is suppressed by p38 activity, but requires GSK-3 activity. Furthermore, *Lpl* expression is regulated by p38 and GSK-3 signalling. This is the first study demonstrating a relationship between PPARγ2 expression and chondrocyte lipid metabolism and its regulation by p38 and GSK-3 signalling.

Keywords: chondrocyte • lipid metabolism • PPARγ • p38 • GSK-3

Introduction

Cartilage forms the template on which bone is modelled, a process termed endochondral ossification. The mesenchymal cells from which chondrocytes derive are pluripotent and have the ability to differentiate into chondrocytes, osteoblasts, myocytes or adipocytes [1]. The molecular cues modulating the development of these mesenchymal cells ultimately determine their final identity and tissue characteristics. Chondrocyte differentiation is accompanied by unique changes in gene expression as cells progress through their life cycle in the growth plate. The Sox and Runx families of transcription factors control progression through the chondrocytic lineage, promoting cell condensation, proliferation and finally hypertrophy within a calcified, mineral matrix which the chondrocytes themselves produce [2]. The balance between proliferation and hypertrophy is finely tuned by the negative feedback loop of Indian hedgehog (Ihh) and parathyroid hormone-related peptide (PTHrP). Ihh, produced by pre-hypertrophic chondrocytes, induces PTHrP expression that prevents cells from initiating differentiation (reviewed in: [3-5]). Bone morphogenetic proteins and Wnts are also produced by hypertrophic chondrocytes and act in synergy with Ihh to induce osteogenesis of adjacent cells [5]. Various intracellular signalling pathways play a role in directing gene expression and regulate chondrocyte differentiation. These pathways include p38 MAPK [6-8] and GSK-3β [9].

Similar to chondrocytes, the conversion of mesenchymal cells to adipocytes and osteoblasts requires molecular cues. The nuclear receptor peroxisome proliferator activated receptor (PPAR)γ2 is a critical regulator of adipogenesis (reviewed in [10, 11]). Activation of this transcription factor favours

*Correspondence to: Frank BEIER,
Canada Research Chair in Musculoskeletal Health,
CIHR Group in Skeletal Development and Remodelling,
Department of Physiology and Pharmacology,
University of Western Ontario, London,
Ontario N6A 5C1, Canada.
Tel.: 519 661 2111 85344
Fax: 519 661 3827
E-mail: fbeier@uwo.ca

doi:10.1111/j.1582-4934.2008.00396.x

adipogenesis above osteogenesis of mesenchymal stem cells. This was demonstrated by Akune *et al.* [12] who described increased osteoblastogenesis *in vitro* and higher trabecular bone volume *in vivo* as a result of PPARγ insufficiency. PPARγ is a member of the PPAR family of nuclear receptors, for which three members have been identified: PPARα, PPARβ/δ and PPARγ. These three factors are products of different genes and are implicated in various aspects of lipid and energy metabolism. PPARα has been most studied for its role in fatty acid catabolism in the liver, but is also expressed in other tissues including heart, skeletal muscle, kidney, brown fat [13–15] as well as chondrocytes [16]. PPARβ/δ is expressed ubiquitously [13, 17] and appears to be involved in fatty acid oxidation [18]. Unlike its relatives, PPARγ exists as two isoforms, PPARγ1 and PPARγ2. Both proteins are the product of the same gene, but arise from the use of different promoters. PPARγ2 has an additional 28 (human) or 30 (mouse) amino acids at the NH_2-terminal end [19–25]. In addition to a dissimilar protein structure, these isoforms also display distinct expression patterns. PPARγ2 is mainly expressed by adipose tissue, whereas PPARγ1 displays ubiquitous expression [26, 27]. PPARγ has been best described for its role in adipogenesis and lipid storage [28], although recent studies have shown that PPARγ also participates in cellular differentiation, inflammatory responses and apoptosis. Furthermore, numerous pathological conditions, including cancer, atherosclerosis and diabetes, are accompanied by altered PPARγ levels and activity (reviewed in: [29–31]).

The expression of PPARγ2 was first described in chondrocytes by Bordji *et al.* [32] who described that activation of PPARγ suppresses interleukin-1β effects on nitric oxide production and proteoglycan synthesis. More recently, Shao *et al.* [16] described expression of all three PPARs in growth plate chondrocytes. Although the function of PPARγ in chondrocytes remains largely unknown, it has been shown that activation of PPARγ inhibits T_3-induced terminal differentiation and promotes apoptosis [33]. PPARγ activity has also been shown to suppress TGF-β induction of proteoglycan production [34] and to act as an anti-inflammatory agent in osteoarthritis [35]. These numerous functions have been suggested to be possible because of its wide range of ligands [36].

Because chondrocytes are not readily presumed to be lipid storage or metabolizing cells, their lipid metabolism has been poorly investigated, though they are capable of lipid metabolism [37]. The aim of the present study was to explore the role of PPARγ in chondrocytes, analyse the lipid metabolic capacity of chondrocytes, and look at possible signalling pathways involved in the responses elicited by PPARγ activation. We show that PPARγ2 expression is spatially and temporally controlled during chondrocyte differentiation. However, PPARγ activation does not appear to significantly alter bone growth or differentiation of chondrocytes, although it does play a major role in regulating the lipid storage capacity of chondrocytes. These effects are mediated *via* GSK-3 signalling and to a lesser extent involve p38 activity.

Methods and materials

Materials

Timed pregnant CD1 mice [at 11.5 d.p.c (days after coitum) and 15.5 d.p.c] were purchased from Charles River Laboratories (St Constant, Quebec, Canada). All animal studies were conducted in accordance with protocols approved by the Animal Use and Care Committee of the University of Western Ontario. All cell culture reagents were from Invitrogen (Burlington, ON, Canada) unless stated otherwise. PD169316 [4-(4-fluorophenyl)-2-(4-nitrophenyl)-5-(4-pyridyl)-1H-imadazole] was from Calbiochem (San Diego, CA, USA). Monoclonal anti-collagen type X, SB216763, Mayers-haematoxylin and oil red O were from Sigma-Aldrich (Mississauga, ON, Canada). Troglitazone was from Cayman Chemicals (Burlington, ON, Canada). The anti-PPARγ2 antibody and blocking peptide were from Santa Cruz Biotechnology, Inc. (Santa Cruz, CA, USA). Faramount mounting media, rabbit- and goat-serum were from DakoCytomation (Mississauga, ON, Canada). All other reagents were of analytical grade from commercial suppliers.

Chondrocyte micromass isolation and culture

Chondrocytes for micromass culture were isolated from hindlimb paddles of CD1 mouse embryos at 11.5 d.p.c as previously described [38]. The cell density was adjusted to 2.5×10^7 cells/ml before seeding in 10-μl droplets per well in Nunc 24-well plates. After allowing the cells to adhere for 1 hr at 37°C with 5% CO_2, they were fed with differentiation media that consisted of DMEM:F12 (2:3), 10% FBS, 0.5 mM L-glutamine, penicillin (25 units/ml), streptomycin (25 μg/ml), 0.25 mM ascorbic acid and 1 mM β-glycerophosphate. The day of isolation was considered as day 0. Media were replenished daily with p38 and GSK-3 inhibitor supplementation from day 2. The p38 inhibitor, PD169316, and GSK-3 inhibitor, SB216763, were used at 10 μM unless indicated otherwise. Inhibitors were resuspended in DMSO and therefore control cells received equivalent volumes of vehicle (DMSO). The DMSO concentration did not exceed 0.1% of the medium volume.

Monolayer culture of primary chondrocytes

Chondrocytes for monolayer culture were obtained from 15.5 d.p.c. mouse embryos as previously described with minor variations [6]. Briefly, bones (tibiae, femurs, humeri) were separated and cleaned of connective tissue and incubated overnight at 37°C in media consisting of α-MEM supplemented with 0.25 mM ascorbic acid, 1 mM β-glycerophosphate, 0.2% bovine serum albumin, 0.5 mM glutamine, 40 units penicillin/ml and 40 μg streptomycin/ml. The bones were then washed with Puck's solution A (PSA) (0.5 g KCl/l, 8 g NaCl/l, 0.35 g $NaHCO_3$/l, 1 g glucose/l) before incubating with gentle rocking for 15 min. in 1× Trypsin-EDTA (ethylenediaminetetraacetic acid) at 37°C. Following two washes with PSA, the bones were further digested with 0.3% (w/v) collagenase-P (Roche, Mississauga, ON, Canada) in DMEM for 2 hrs at 37°C with gentle agitation. Digested cells were collected by centrifugation at 200 × *g* for 5 min. The collagenase supernatant was removed and the cells were resuspended in differentiation media as used for micromass chondrocytes. The cell suspension was passed through a 40-μm cell sieve and then plated in monolayer in Nunc multiwell plates at 8×10^4 cells/cm^2. Cells were fed every 2 to 3 days

with differentiation media (as for micromass cultures) supplemented with inhibitors of p38 (PD169316), GSK-3 (SB216763) (both at 10 (M) or PPARγ agonist (troglitazone at 2.5 (M) from day 1. The day of plating into multiwell plates was considered as day 0.

Metatarsal organ culture

Metatarsals were dissected from embryonic 15.5 d.p.c. mouse embryos and either snap-frozen on dry ice for cryosectioning, or maintained in media comprising α-MEM supplemented with 0.25 mM ascorbic acid, 1 mM β-glycerophosphate, 0.2% bovine serum albumin, 0.5 mM glutamine, 40 units penicillin/ml and 40 μg streptomycin/ml. Media were not changed, although test agents were added daily at concentrations used for monolayer chondrocytes. After 72 hrs of treatment, metatarsals were either harvested for protein and western blot analysis or fixed for sectioning with 4% paraformaldehyde for 2 hrs. These fixed samples were stored in 10% neutral buffered formalin until they could be embedded in paraffin and sectioned.

Microdissected tibiae

Immediately following sacrifice of 15.5 d.p.c. mouse embryos were immediately removed and freed from soft tissue. The tibiae were separated under a Zeiss (Toronto, ON, Canada) dissecting microscope into three zones: resting/proliferative, hypertrophic and mineralized region. The mineralized region was discarded but the resting/proliferative and hypertrophic zones were each pooled from the embryos of four pregnant mice. RNA was isolated using the RNeasy® Lipid Tissue Extraction protocol according to the manufacturer's instructions (Qiagen, Mississauga, Canada). RNA integrity was verified as described by Agoston *et al.* [39]. These experiments were repeated four independent times.

RNA isolation and real-time PCR

RNA isolation and real-time PCR was performed as previously described [38]. Real-time PCR was performed with the TaqMan one-step master mix kit (Applied Biosystems, Streetsville, ON, Canada) with gene-specific target primers and probes. All samples were amplified in three parallel reactions in the ABI Prism 7900 Sequence Detection System (Applied Biosystems). Experiments were performed from three or more independent cell preparations, with similar results. Primers and probes for *osteocalcin* (*OCN*) (forward primer 5′-CCTGAGTCTGACAAAGCCTTCA, reverse primer 5′-GCCGGAGTCTGTTCACTACCTT and probe 6-FAM-5′-TCCAAGCAGGAGGGCA-MGBNFQ) and *collagen X* gene (forward primer 5′-ACGCCTACGATGTACACGTATGA, reverse primer 5′-ACTCCCTGAAGCCTGATCCA and probe 6-FAM-5′-AGTACAGCAAAGGCTAC-MGBNFQ) were designed using the software PrimerDesigner 2.0 (Applied Biosystems). The primers and probes used to detect glyceraldehyde-3-phosphate dehydrogenase (GAPDH) were from the TaqMan GAPDH control reagents (forward primer 5′-GAAGGTGAAGGTCGGAGTC; reverse primer 5′-GAAGATGGTGATGGGATTTC; probe JOE-CAAGCTTCCCGTTCTCAGCC-TAMRA). *Ihh*, *Runx2*, *osterix* (*Osx*), *PPARγ2*, *Fabp4*, and *Lpl* probe sets were purchased as Assay-on-demand™ gene expression products (Applied Biosystems) and used according to manufacture's instructions. Transcript quantity was determined from standard curves and the relative amount of gene transcript present in a sample was calculated and normalized by dividing the value calculated for the gene of interest by the value calculated for the house-keeping gene.

Immunohistochemical analysis

Three-micrometre metatarsal sections were deparaffinized in xylene, rehydrated through graded ethanols and processed for antigen localization as previously described with minor variations [40]. Antigen retrieval for collagen X was performed by incubating the sections with protease (EC 3.4.24.31) from *Streptomyces griseus* (5.2 units/mg/ml) (Sigma-Aldrich) for 10 min. at room temperature. PPARγ2 antigen retrieval was done with 20-min. microwaving in 10 mM citrate buffer (pH 6). Normal rabbit serum (5% in PBS) was used for blocking before incubating with anti-PPARγ2 (G-18) (Santa Cruz Biotechnology, cat # sc-22020) overnight at 4°C. Anti-PPARγ2 was diluted 1:175 (final concentration was 1.1 μg/ml) with 5% serum/PBS. The secondary antibody for PPARγ2 was HrP-conjugated rabbit anti-goat (Santa Cruz Biotechnology) diluted 1:200 with PBS. Anti-collagen X was diluted 1:1000 and incubated overnight after blocking sections in 5% goat serum. The secondary antibody for collagen X was HrP-conjugated goat antimouse (Santa Cruz Biotechnology). Antigen immunolocalization was analysed using horseradish peroxidase-diaminobenzidine (PPARγ2) or 3-amino-9-ethylcarbazole (Collagen X) according to manufacturer's instructions (DakoCytomation). Sections were counterstained with Mayer's haematoxylin and mounted with Faramount. As a negative control, the primary collagen X antibody was omitted, whereas for PPARγ2 competition studies with a blocking peptide was performed according to manufacturer's recommendations (Santa Cruz Biotechnology). These controls showed no signal for either antibody.

Oil red O stain

Chondrocytes, which were prepared, maintained and treated as described under monolayer culture of primary chondrocytes, were seeded on glass cover slips at a density of 80,000 cells/cm^2. After 8 days in culture, the cells were fixed in 4% paraformaldehyde, rinsed well with water and then stained for lipids with oil red O. Oil red O staining in metatarsals and tibiae were performed on freshly isolated, snap-frozen specimens. Following cryosectioning, sections were allowed to equilibrate to room temperature before staining with oil red O. Sections were mounted with Faramount. Monolayer cultures were analysed for lipid droplet size and number on a Leica microscope by a blinded investigator. Ten independent fields per slide were counted and averaged per experiment. The experiment was repeated five independent times.

Western blot analysis

Immunoblot analysis of collagen X was performed on metatarsals treated for 72 hrs with PPARγ agonist, troglitazone. Metatarsals were harvested, washed twice with ice-cold phosphate buffered saline before suspending in RIPA buffer supplemented with protease inhibitor cocktail I (Sigma-Aldrich), inhibitor set IV (Calbiochem) and complete mini tablet (Roche Molecular Biochemicals). After snap-freezing on dry ice, the samples were sonicated and centrifuged at 10,000 × *g* for 10 min. The supernatants were analysed for protein content using the BCA method and then stored at −20°C until required. Twenty micrograms of protein from each sample

was prepared according to manufacturer's instructions for loading onto the Bis-Tris pre-cast gel system (Invitrogen). Samples were run under reducing conditions, before transferring to polyvinylidene difluoride membrane (BioRad, Mississigua, ON, Canada). The membranes were saturated by incubation for 2 hrs at room temperature in Tris-buffered saline/Tween buffer containing 5% bovine serum albumin. The membranes were then incubated overnight at 4°C with antimouse collagen X (1:1000). After washing in Tris-buffered saline/Tween buffer, the membranes were incubated with secondary antibody that was visualized by the West Femto Maximum Sensitivity Substrate™ kit (Pierce, Nepean, ON, Canada). Equal loading of the blot was assessed by reprobing with anti-β-actin.

Statistical analysis

Data are expressed as means ± S.E.M. from at least three independent cell preparations. Student's t-test and ANOVA were used to determine significance, which was considered to be $P < 0.05$. Correlations were calculated using the GraphPad Prism software.

Results

PPARγ2 expression is regulated during chondrocyte differentiation

Our first aim was to elucidate PPARγ2 expression patterns within the embryonic growth plate and establish possible signalling pathways regulating these patterns. PPARγ2 immunoreactivity in freshly dissected 15.5 d.p.c. mouse embryo metatarsals was weak (Fig. 1A) but became clearly noticeable by 16.5 d.p.c. (Fig. 1B) and 17.5 d.p.c. (Fig. 1C). Metatarsals from 15.5 d.p.c. embryos that were maintained in culture for 3 days demonstrate convincing signal in pre-hypertrophic/hypertrophic chondrocytes (Fig. 1D). In contrast to 15.5 d.p.c. metatarsals, PPARγ2 is detectable in freshly harvested 15.5 d.p.c. tibiae, localizing to pre-hypertrophic and hypertrophic chondrocytes (Fig. 1E). The signal intensity in tibiae increases at 16.5 d.p.c. and by 17.5 d.p.c. the signal localizes to a small band of pre-hypertrophic cells (Fig. 1F). This developmental expression was confirmed at the transcript level using RNA extracted from freshly microdissected 15.5 d.p.c. tibiae, demonstrating that the hypertrophic zone expresses significantly greater *PPARγ2* mRNA levels compared to the resting/proliferative zone (Fig. 1G).

Both monolayer chondrocyte and three-dimensional micromass cultures have been extensively used to address and investigate the differentiation of chondrocytes *in vitro*. We used both models to compare and examine the transcript expression patterns of *PPARγ2*. Our data demonstrate that *PPARγ2* transcript expression increases as monolayer (Fig. 1H) and micromass (Fig. 1I) chondrocytes differentiate in culture. Monolayer chondrocyte cultures demonstrate increasing transcript levels with time in culture, whereas micromass cultures demonstrate a rapid acquisition of transcript level between days 3 and 6, which then plateaus. Taken together, these results demonstrate that chondrocytes express *PPARγ2* in a pattern that is temporally and spatially regulated within growth plate chondrocytes.

The p38 MAPK and GSK-3 signalling pathways have been implicated in controlling chondrocyte differentiation [6–9, 38]. We therefore next addressed whether either of these signalling pathways affect *PPARγ2* expression. Using pharmacological inhibitors of p38 (PD169316) and GSK-3 (SB216763) in both monolayer and micromass chondrocyte cultures, we show that by the end of the culture period, *PPARγ2* transcript levels are significantly elevated with p38 inhibition, whereas GSK-3 inhibition leads to a significant reduction in *PPARγ2* transcript expression (Fig. 1H and I). These data therefore show that p38 activity acts to suppress *PPARγ2* transcript expression levels in growth plate chondrocytes, whereas expression levels require GSK-3 activity.

Metatarsal bone growth is unaffected by the PPARγ agonist, troglitazone

PPARγ has been implicated in numerous functions including inhibition of T_3-induced chondrocyte differentiation [33]. As the roles in chondrocytes have not been fully addressed, our next aim was to address whether PPARγ participates in chondrocyte growth. Exposing metatarsals to the PPARγ agonist, troglitazone, for 72 hrs did not modify metatarsal growth from control bones (Fig. 2A), suggesting that PPARγ does not affect endochondral bone growth. Furthermore, the length of the hypertrophic zone and hypertrophic cell size were not significantly altered by PPARγ agonist treatment (data not shown). In addition, histological analysis of these sections did not display any variation in response to PPARγ agonist treatment (Fig. 2B). These data suggest that although PPARγ expression increases with differentiation, it does not affect growth of metatarsals in culture.

PPARγ affects expression of selected chondrocyte-specific genes

We next asked whether PPARγ activation affects expression of chondrocyte markers. Due to PPARγ2 expression in pre-hypertrophic/hypertrophic chondrocytes, we examined *Ihh* transcript levels in treated monolayer cultures. PPARγ was activated with troglitazone for 8 days, after which *Ihh* transcript expression was observed to be significantly elevated compared to DMSO treated chondrocytes (Fig. 3A). In contrast, transcript levels of the hypertrophic marker collagen were reduced in response to PPARγ activation in monolayer cells (Fig. 3B). Collagen X protein levels from metatarsals treated with troglitazone for 72 hrs mirrored the transcript level trends as determined from Western blot images (Fig. 3C) by spot densitometry (Fig. 3D), although the effects on collagen X protein were relatively mild. These results suggest that

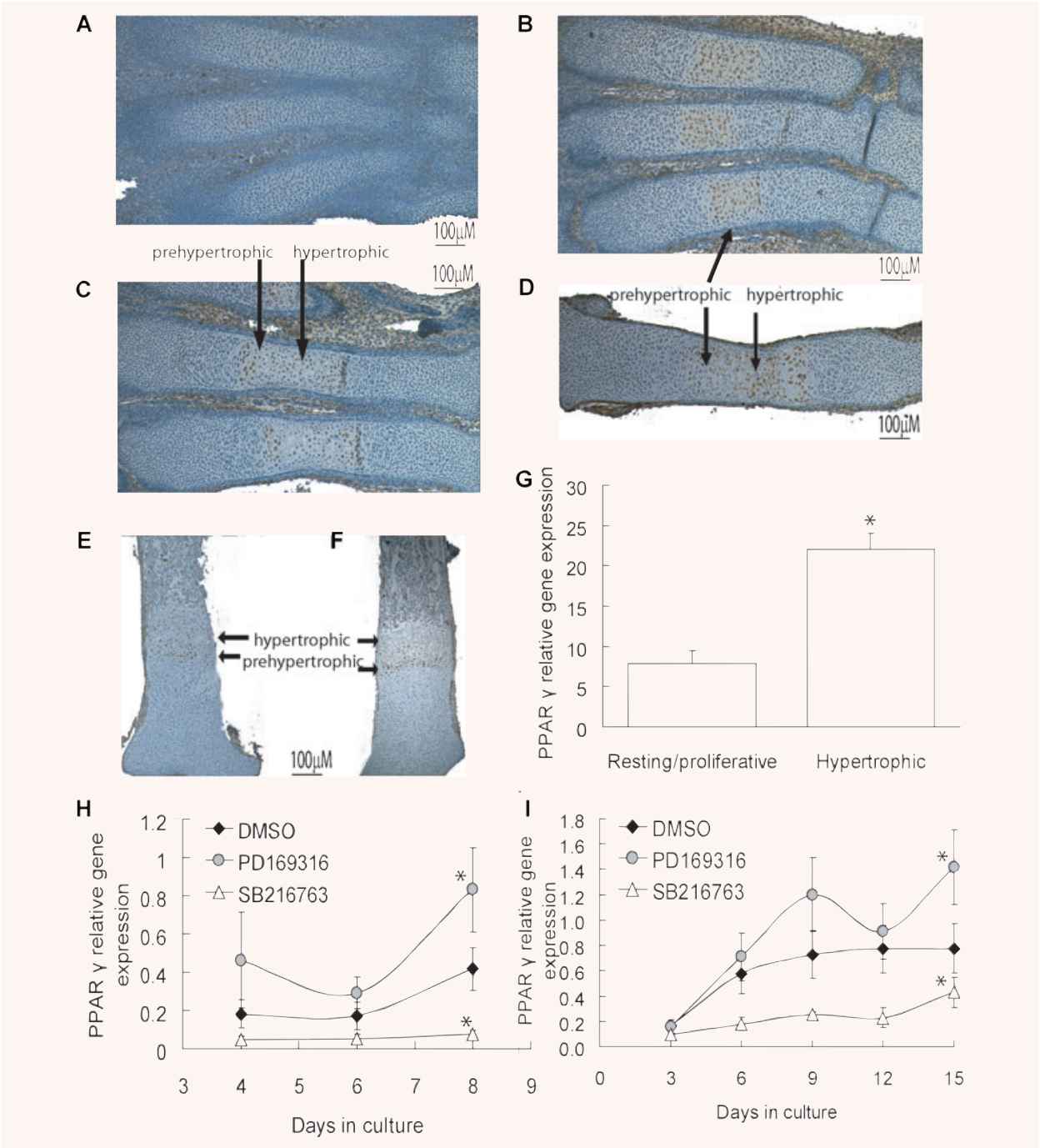

Fig. 1 PPARγ2 expression in chondrocytes. Immunohistochemical localization of PPARγ2 in freshly dissected metatarsals from 15.5 d.p.c. embryos (**A**), 16.5 d.p.c. embryos (**B**), 17.5 d.p.c. embryos (**C**), metatarsals from 15.5 d.p.c embryos but maintained in culture for 72 hrs (**D**), as well as tibiae from freshly dissected 15.5 d.p.c. embryos (**E**) and 17.5 d.p.c. embryos (**F**). Cellular localization is indicated by the brown substrate. Magnification = 100×. (**G**) Total RNA was isolated from microdissected tibiae and analysed for *PPARγ2* transcript levels by real-time PCR. (**H**) Monolayer and (**I**) micromass chondrocytes were cultured as described in the presence and absence of 10 (M p38 inhibitor (PD169316) or GSK-3 inhibitor (SB216763) and harvested for *PPARγ2* transcript analysis by real-time PCR at the indicated times. Values are means ± S.E.M. of four independent chondrocyte cultures. The symbol '*' indicates significance of at least $P < 0.04$ compared to control cells at the indicated time-point.

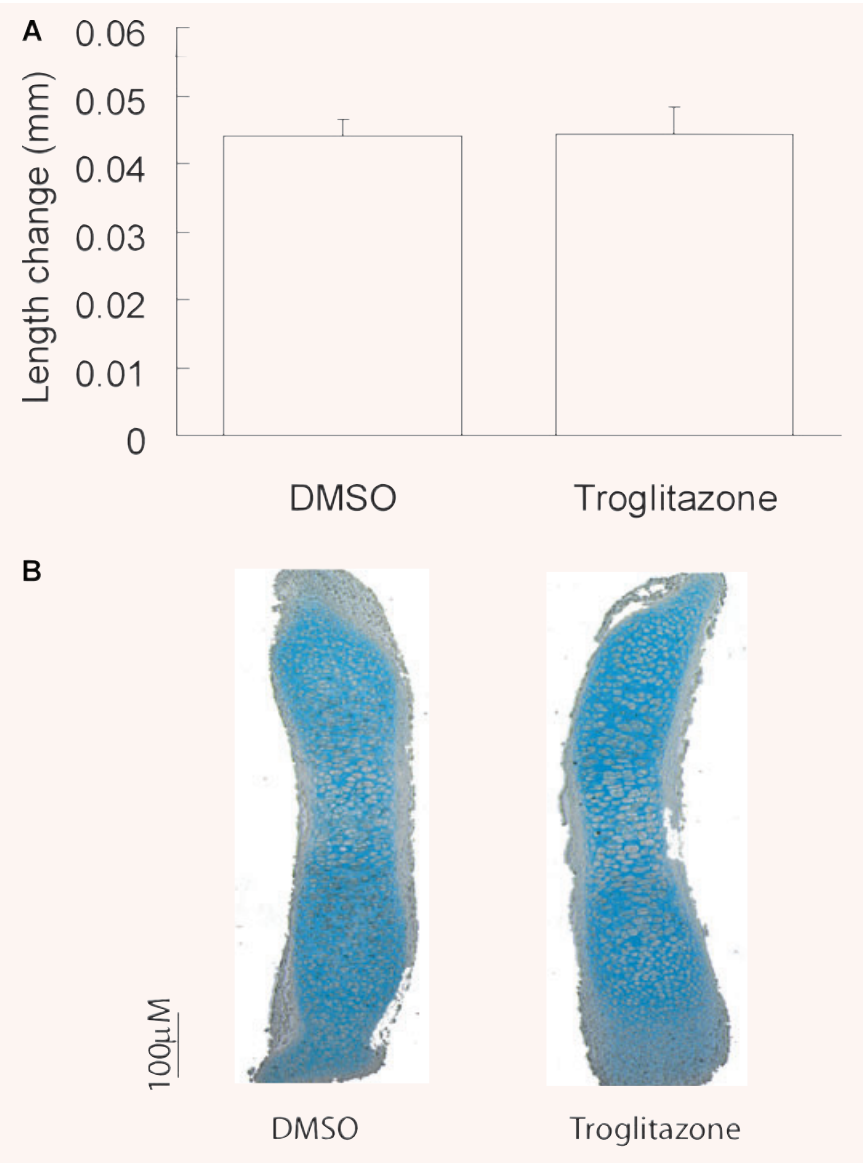

Fig. 2 The effect of activating PPARγ on growth and histology of metatarsals. Metatarsals were harvested from 15.5 d.p.c. embryos and maintained in culture as described with 72 hrs exposure to 2.5 μM troglitazone. (**A**) The change in length over 72 hrs was determined by measuring the length of the metatarsals after isolation, and again after 72 hrs of treatment. The values represent the change in length over the 72-hrs period. (**B**) Metatarsals were sectioned and stained with alcian blue. Histology of the sections was recorded on a Leica microscope at 100× magnification. Values represent the mean ± S.E.M. of eight independent chondrocyte cultures.

PPARγ may inhibit chondrocyte maturation from the pre-hypertrophic to the hypertrophic stage. These results are in agreement with those of Shao *et al.* [41] and Wang *et al.* [42] who described inhibited T_3-induced hypertrophic differentiation by PPARγ agonists.

PPARγ has been noted in numerous papers to promote adipocyte differentiation at the expense of osteogenesis [12, 43–45]. We have previously shown that chondrocyte cultures are capable of expressing osteoblast-associated genes, including *Runx2*, *Osx* and *OCN* [6]. As p38 inhibition has been shown to increase *PPARγ2* expression (Fig. 1E and F), as well as *Runx2*, *Osx* and *OCN* [6], we next asked whether PPARγ activation affected expression of these genes. Using monolayer chondrocyte cultures we show that although increases in *Runx2* and *Osx* transcript expression upon treatment with troglitazone for 8 days were not significant, *OCN* expression levels were significantly elevated in response to activation of PPARγ with troglitazone (Fig. 4). These data suggest that osteoblast-associated gene expression in chondrocyte cultures is affected by PPARγ activity.

We next asked whether p38 and PPARγ cooperate in regulating *Runx2*, *Osx* and *OCN* transcript expression. Simultaneous inhibition of p38 activity with PPARγ activation did not significantly affect

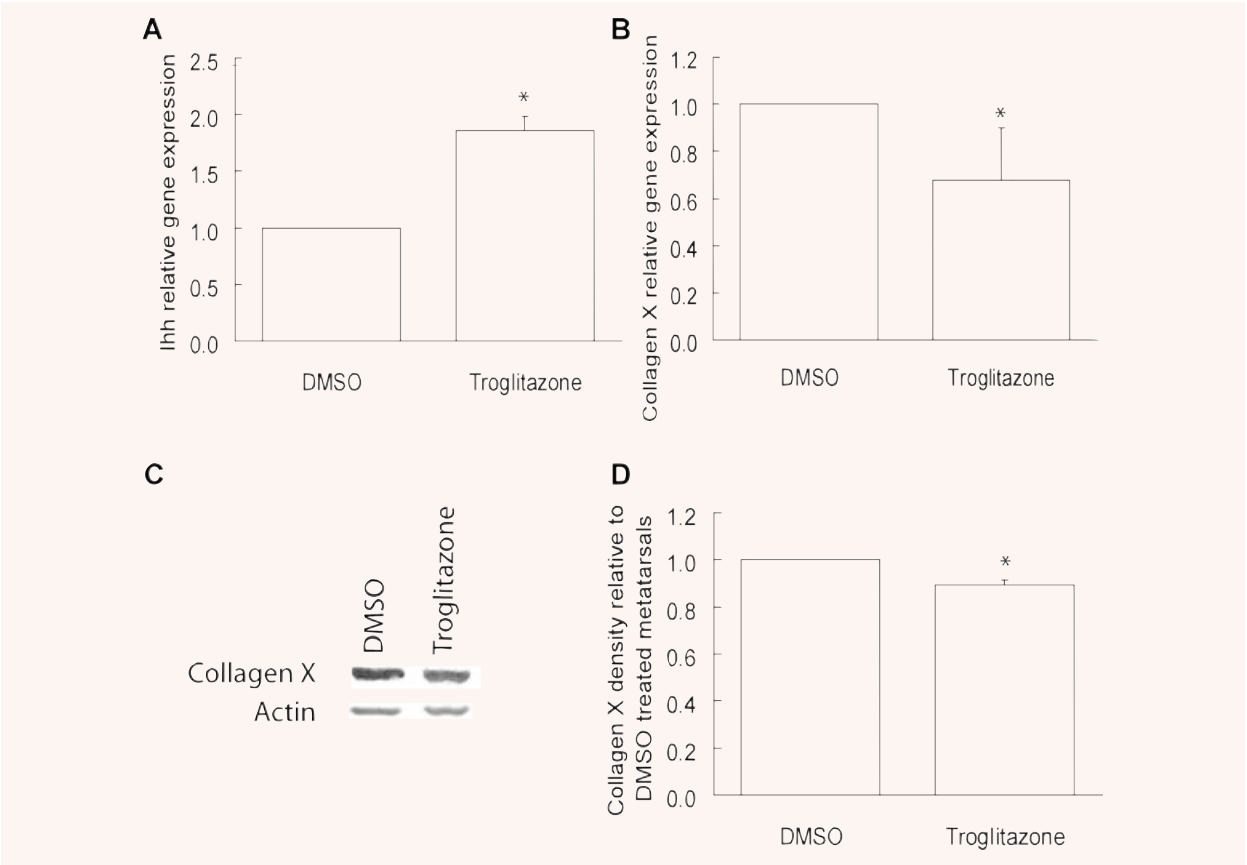

Fig. 3 Chondrocyte markers are regulated in response to changes in PPARγ activation. Monolayer chondrocytes were treated for 8 days with 2.5 μM troglitazone before RNA was harvested and analysed for transcript expression of (**A**) *Ihh* and (**B**) *collagen X*. (**C**) Expression trends of collagen X protein was confirmed by western blot analysis from 72-hr treated cultures. (**D**) Spot densitometry of western blots was performed. Values are mean ± S.E.M. from three independent chondrocyte cultures. The symbol '*' indicates significance of at least $P < 0.01$ compared to control cells.

Runx2 and *Osx* expression compared to troglitazone treatment alone (Fig. 4). However, *Runx2* and *Osx* transcripts were significantly reduced when compared to p38 inhibition alone, unlike *OCN* levels that remained unaltered between p38 inhibition alone and simultaneous activation of PPARγ with p38 inhibition. These results suggest that p38 and PPARγ pathways cross-talk to regulate *Runx2* and *Osx* transcript levels, but also emphasize the complexity in the signalling networks regulating chondrocyte gene expression.

We also asked whether GSK-3 and PPARγ signalling pathways cooperate to influence *Runx2*, *Osx* and *OCN* gene expression. Inhibition of GSK-3 resulted in significantly reduced levels of all three genes (Fig. 4). Effects of PPARγ on the three genes were abolished by GSK-3 inhibition, suggesting GSK-3 activity is required for appreciable expression of the osteoblast-associated genes under basal conditions, as well as PPARγ-induced (troglitazone treated) osteoblast-associated gene expression in chondrocyte monolayer cultures.

PPARγ affects chondrocyte lipid metabolism through GSK-3β signalling

Over recent years PPARγ has been described to participate in numerous cellular functions including cell differentiation, apoptosis, insulin sensitivity and lipid storage. For this reason we next investigated whether PPARγ contributes to lipid metabolism within differentiating chondrocytes. Lipid metabolism has not been well described in chondrocytes, although in 1982 Kirckpatrick *et al.* [37] showed that chondrocytes contain lipid droplets perinuclear and peripherally. In fresh frozen sections from metatarsals and tibiae isolated from 15.5 d.p.c. embryos, we noticed lipid staining in the pre-hypertrophic and hypertrophic zone, as determined by oil red O stained droplets (Fig. 5). Monolayer chondrocytes also demonstrate the capacity to accumulate lipid droplets with time in culture, as demonstrated by oil red O staining

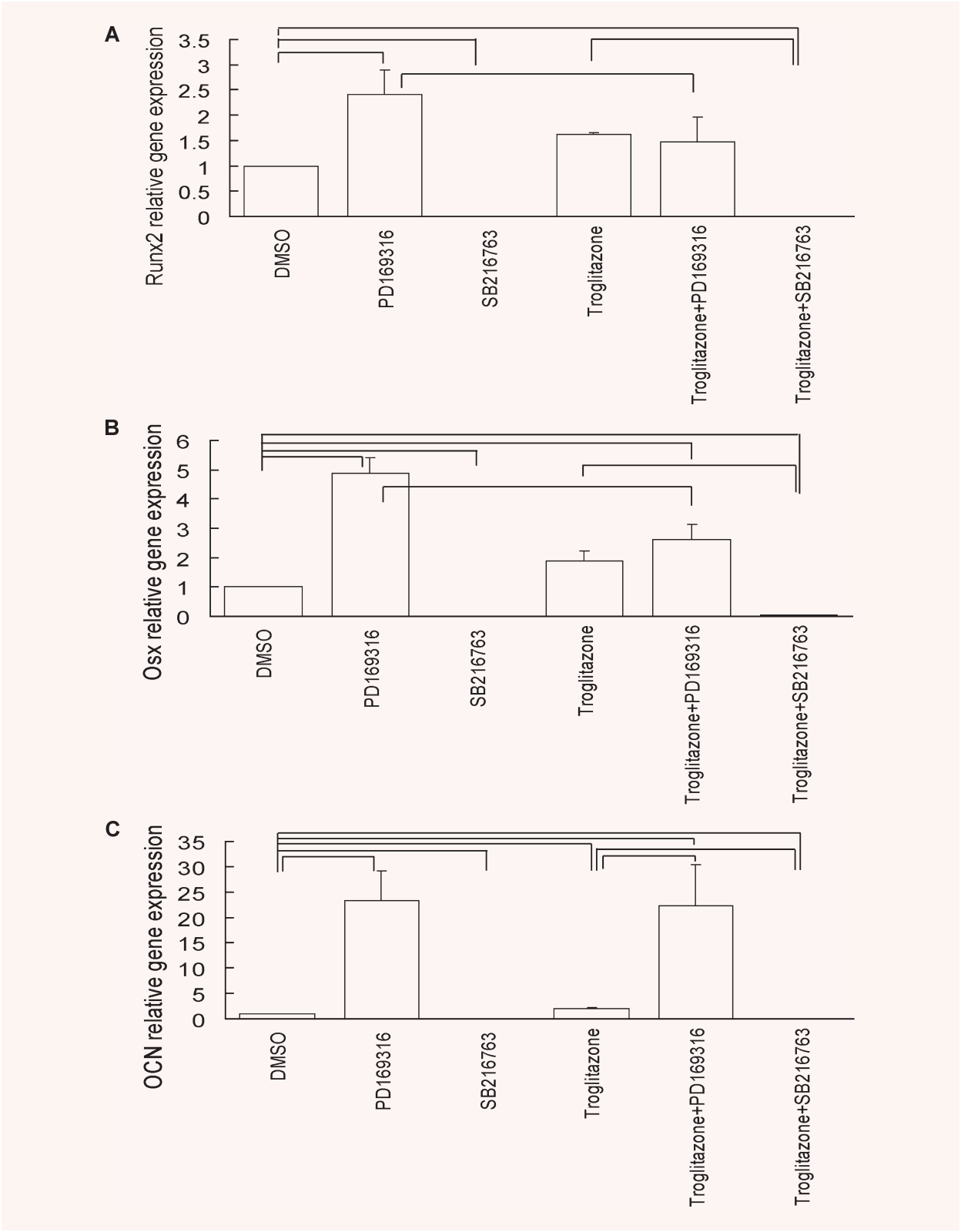

Fig. 4 Hypertrophic- and osteoblast-associated gene expression in response to PPARγ activity changes. Monolayer chondrocytes were treated for 8 days with 2.5 μM troglitazone in the presence or absence of p38 (PD169316) and GSK-3 (SB216762) inhibitors. RNA was harvested and analysed by real-time PCR for (**A**) *Runx2*, (**B**) *Osx* and (**C**) *OCN* transcript levels. Values are mean ± S.E.M. from three independent chondrocyte cultures. Significance of at least $P < 0.05$ between treatments are indicated by the lines.

(Fig. 6A). These results reveal that chondrocytes are capable of lipid accumulation and storage.

To examine whether PPARγ regulates lipid metabolism in chondrocyte cultures, monolayer chondrocyte cultures were exposed to troglitazone for 8 days and then stained with oil red O. PPARγ activation resulted in copious amounts of oil red O stained droplets (Fig. 6A). Quantitative analyses showed that both size (Fig. 6B) and number (Fig. 6C) of these droplets were markedly increased from control cultures.

We next asked whether the observed lipid accumulation in chondrocytes in response to PPARγ activation involves GSK-3 and/or p38 signalling. Pharmacological inhibitors of p38 and GSK-3 were used simultaneously with troglitazone. The p38 or GSK-3 inhibition resulted in a reduction of PPARγ effects on lipid droplet size (Fig. 6A and B). The number of lipid droplets in monolayer chondrocytes exposed to simultaneous treatment of p38 inhibition and troglitazone treatment resulted in fewer droplets per cell compared to PPARγ activation alone. However, when GSK-3 was inhibited with simultaneous PPARγ activation, the number of lipid droplets per cell was reduced further to levels similar to DMSO treated cultures. Taken together, these data suggest that GSK-3 activity, and to a lesser extent p38 activity, is required for PPARγ-dependent lipid accumulation in chondrocytes.

Lipid-associated genes in chondrocytes are subject to expression regulation by p38 and GSK-3

Because our results showed that PPARγ activation controls lipid metabolism in chondrocytes, we next examined the expression of genes involved in this process. Lipoprotein lipase (*Lpl*) is a well-accepted downstream target gene of PPARγ in lipid metabolism. To confirm that PPARγ is functional and affecting lipid metabolism in chondrocytes, we investigated chondrocyte *Lpl* expression by real-time PCR. The resting/proliferative chondrocyte zone of microdissected tibiae expressed lower transcript levels compared to the hypertrophic region, similarly to *PPARγ2* (Fig. 7A). *Lpl* transcript levels also increased over time in monolayer (Fig. 7B) and micromass (Fig. 7C) cultures, again similar to *PPARγ*. Investigating the effect of p38 and GSK-3 activity on *Lpl* expression by pharmacological inhibitors in both monolayer (Fig. 7B) and micromass (Fig. 7C) cells demonstrates significantly increased expression of *Lpl* with p38 inhibition, whereas GSK-3 inhibition results in significantly reduced expression by the end of the time course. These effects are dose dependent for GSK-3 inhibition (Fig. 7D). These trends mirror those of PPARγ2 expression. Furthermore, activation of PPARγ in chondrocyte cultures leads to elevated fatty acid binding protein 4 (*Fabp4*) (Fig. 7E) and *Lpl* (Fig. 7F) gene expression in monolayer cultures. Taken together, these results demonstrate that chondrocytes are capable of gene expression associated with lipid metabolism and that this expression is regulated by PPARγ activity. Furthermore, PPARγ activity (as determined by *Lpl* expression) is influenced by p38 and GSK-3β activity.

Discussion

The expression pattern of PPARγ was once thought to be restricted to adipocytes. However, PPARγ expression has now been shown in many types of cells including trophoblasts [46], monocytes and macrophages [47], cardiac myocytes [48] and colonic epithelial cells [49]. The expression of PPARγ was first described in chondrocytes by Bordji *et al.* in 2000 [32]. The role of PPARγ, PPARγ and PPARγ receptors in lipid metabolism, regulation of adipocyte proliferation and differentiation, as well as insulin sensitivity, is well accepted [50]. PPARγ is the target of the antidiabetic drugs thiazolinediones (TZDs) and has thus received a great deal of additional investigation, allowing the identification of additional functions including anti-inflammatory actions and regulation of differentiation and apoptosis [47, 51]. Treatment of diabetes with TZDs results in increased insulin sensitivity. It may therefore not be unexpected to observe PPARγ in chondrocytes owing to the importance of insulin for chondrocyte differentiation [52]. In the current study, through the use of specific primer sets in real-time PCR as well as a polyclonal antibody directed towards the PPARγ2 epitope, we demonstrate the expression of *PPARγ2* mRNA and protein in pre-hypertrophic and hypertrophic chondrocytes. Owing to the potent differentiating effect of insulin on chondrocytes, it is tempting to speculate that PPARγ participates in regulating energy metabolism in chondrocytes.

The developmental expression of PPARγ2 is further demonstrated by immunohistochemical staining, where PPARγ2 localized to pre-hypertrophic and hypertrophic chondrocytes. However, Shao *et al.* [16] described expression in all chondrocytes of the rat neonatal tibiae, except the terminally differentiated chondrocytes. Although these results partially contradict the patterns observed by us, there may be numerous reasons for the different result, such as the species and age of the tibiae as well as the antibody and concentrations employed in the immunolocalization of the antigen. The overall conclusion, however, is that chondrocytes do indeed express PPARγ2 in a developmentally regulated pattern.

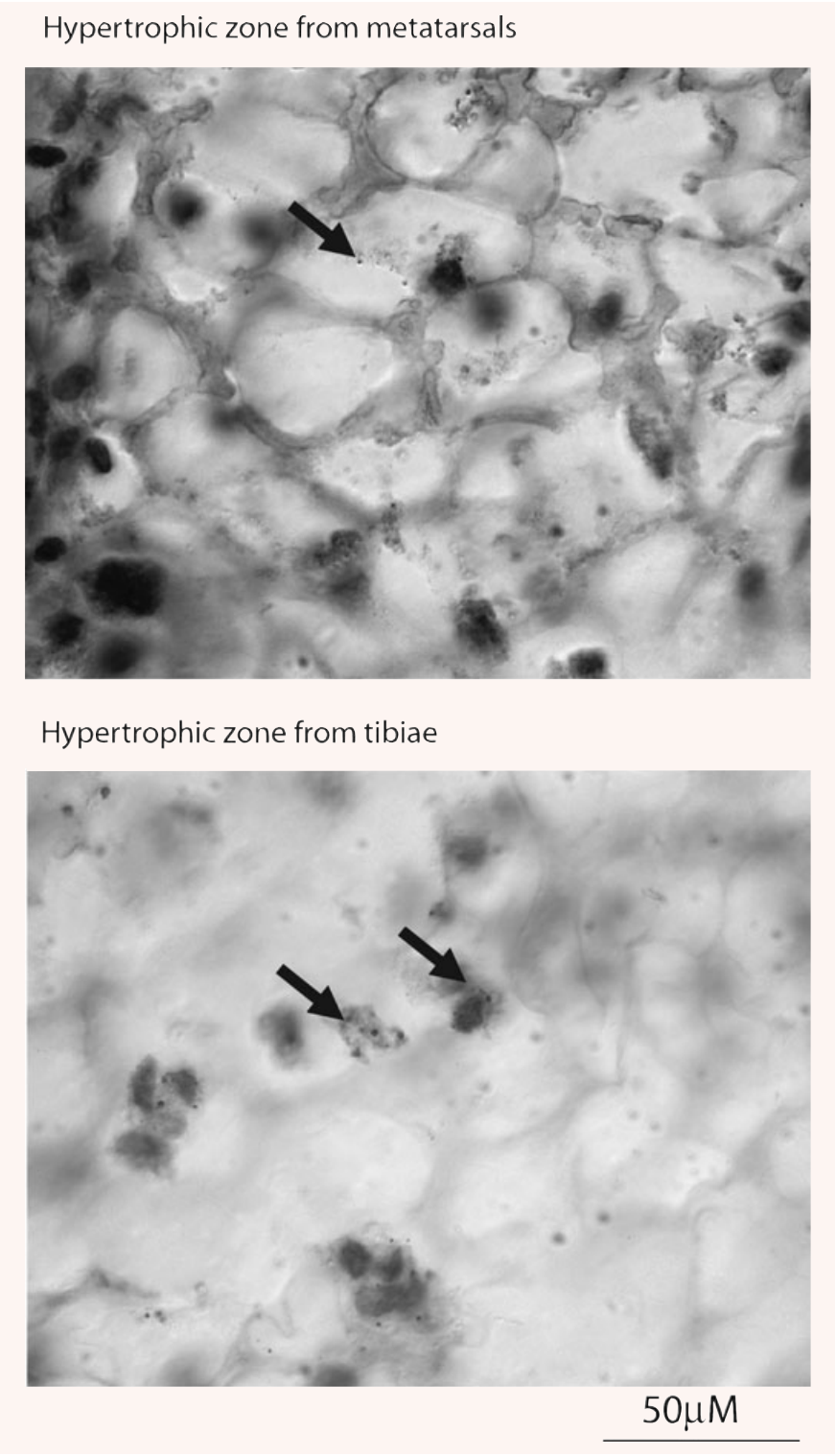

Fig. 5 Oil red O staining in hypertrophic zone chondrocytes. Freshly dissected metatarsals (**A**) and tibiae (**B**) from 15.5 d.p.c. embryos were snap frozen and cryosectioned before being stained with oil red O. Some oil red O positive lipid droplets are indicated by arrows. All specimens were counterstained with haematoxylin. Magnification: 1000×.

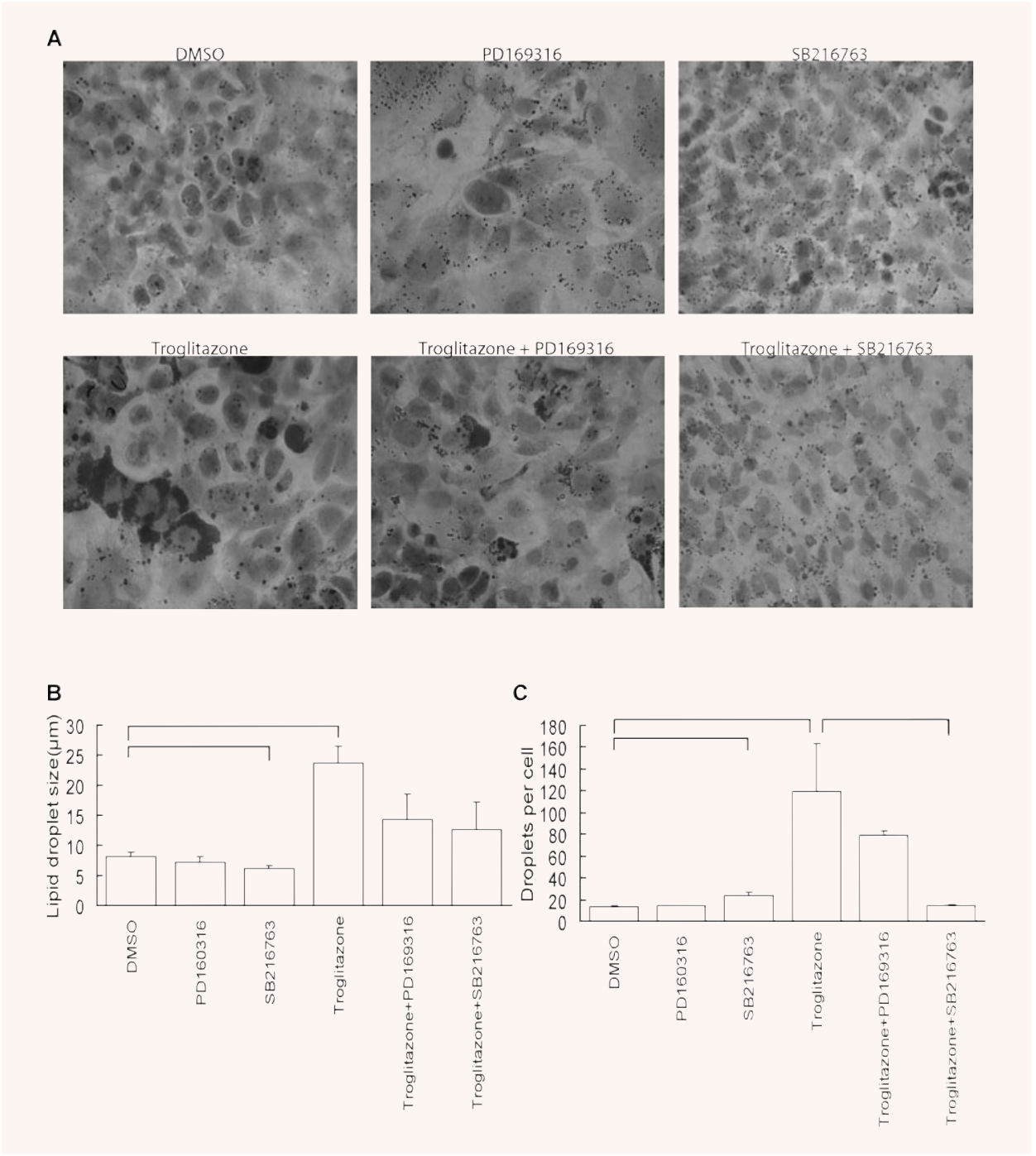

Fig. 6 Oil red O droplets in monolayer chondrocyte cultures. Monolayer chondrocytes were treated for 8 days with DMSO, 10 μM PD169316, 10 μM SB216873, 2.5 μM troglitazone, or troglitazone in combination with PD169316 or SB216763. (**A**) Cells were fixed and stained with oil red O, counterstained with haematoxylin. Magnification: 400×. (**B**) Lipid droplet size was measured on a Leica microscope at 400× magnification, as was the average number of droplets per cell (**C**). Significance between treatments is indicated by bars. Significance observed was at least $P < 0.01$. Experimental numbers are described in the methods.

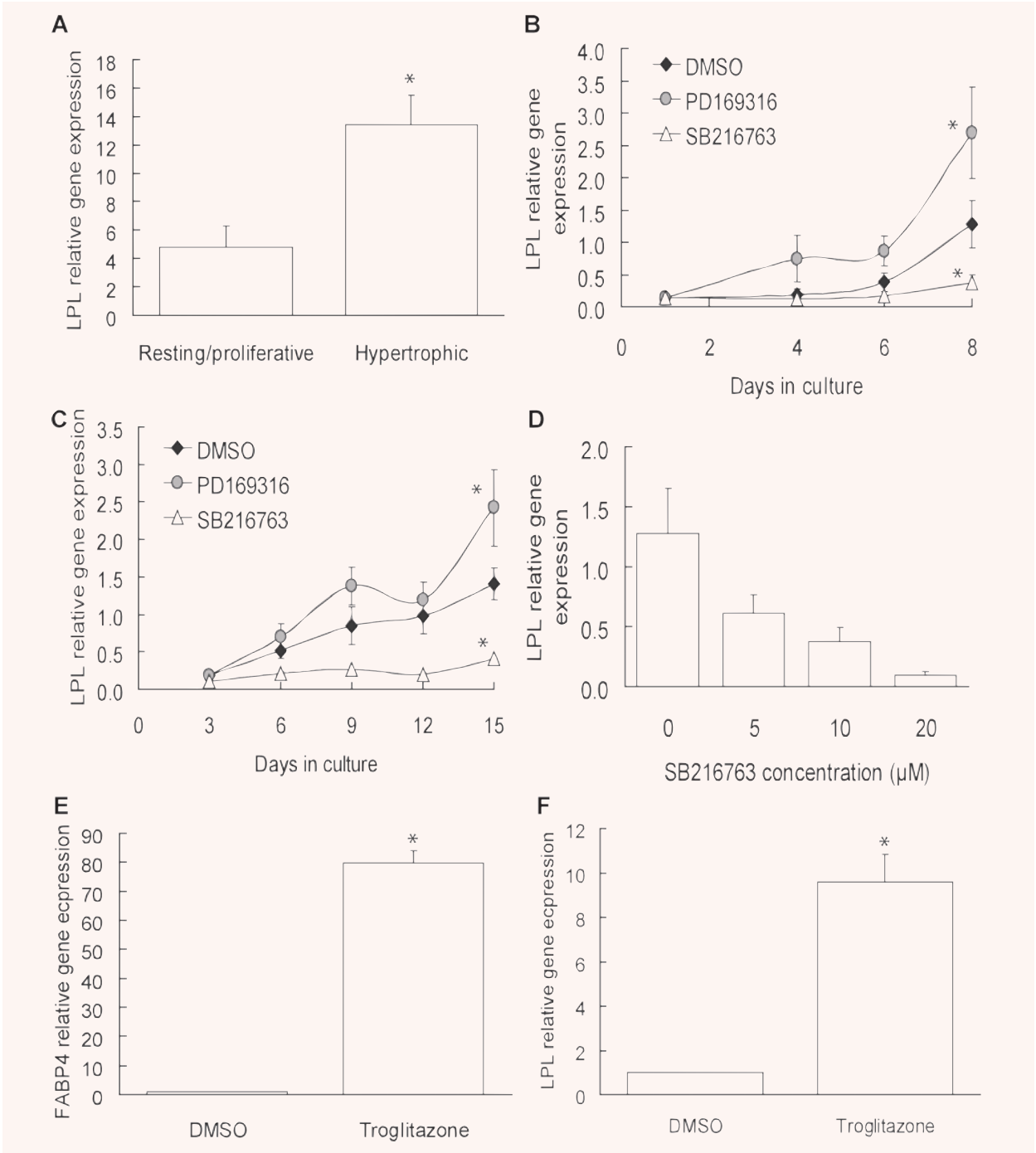

Fig. 7 Lipid-associated gene expression in microdissected tibiae and chondrocyte cultures. (**A**) Total RNA was isolated from microdissected tibiae and analysed for *Lpl* transcript levels by real-time PCR. (**B**) Monolayer and (**C**) micromass chondrocytes were cultured as described in the presence and absence of 10 μM p38 inhibitor (PD169316) or GSK-3 inhibitor (SB216763) and harvested at the indicated times for analysis of *Lpl* transcripts by real-time PCR. (**D**) Monolayer chondrocytes were also exposed to varying concentrations of SB216763 and analysed for *Lpl* transcript levels. *Fabp4* (**E**) and *Lpl* (**F**) transcript levels were determined by real-time PCR in monolayer chondrocytes following an 8-day exposure to 2.5 μM troglitazone. Values represent the mean ± S.E.M. of four independent chondrocyte preparations. The symbol '*' indicates significance of at least $P < 0.05$ compared to control cells.

We found that stimulation of PPARγ did not affect growth of metatarsals in our organ culture system, suggesting that PPARγ does not significantly impact on bone growth. These results support those of Akune *et al.* who found no growth retardation in heterozygous PPARγ knock-out mice [12]. Using markers of chondrocyte differentiation, such as Ihh and collagen X, we showed that PPARγ activation elevates *Ihh* expression while decreasing the hypertrophic marker *collagen X*. These results suggest that PPARγ delays the progression from the pre-hypertrophic to hypertrophic phase.

Our data demonstrate that *PPARγ2* expression in chondrocytes is regulated by various signalling pathways. Both the monolayer and micromass chondrocyte models used in the current study demonstrate that p38 activity in chondrocytes limits PPARγ expression. Regulation of PPARγ by p38 signalling has also been described by Schild *et al*. [46], who demonstrates that in human trophoblasts p38 activity stabilizes PPARγ protein. These authors further observed that mRNA was not significantly affected by p38 activity inhibition, leading them to conclude that p38 regulates PPARγ expression and activity in term human trophoblasts and that cross-talk between p38 and PPARγ signalling may play a role in modulating differentiation and function of the human placenta. However, the current study showed the reverse trend in that inhibition of p38 activity was accompanied by an increase in *PPARγ2* expression and activity. Aouadi *et al*. [53] have shown similar results where p38 activity plays a negative role in adipogenesis by negatively regulating PPARγ. It is interesting to note that many of our previously reported effects of p38 inhibition, such as increased *Ihh*, *Runx2*, *Osx*, *OCN*, and the decreased expression of *collagen X* transcript levels [6], are mirrored by PPARγ activation. It is therefore tempting to speculate that these pathways cross-talk to elicit the observed responses. In addition, the reduction in transcript levels of these genes by simultaneous p38 inhibition and PPARγ activation compared to p38 inhibition alone highlights the complexity of these signalling pathways, as does reduced PPARγ expression on day 12 compared to days 9 and 15 of micromass culture in response to p38 inhibition. The latter defect might be due to stage specific-effects of p38 inhibition on chondrogenic differentiation. For example, the strong induction of PPARγ expression at day 9 by p38 inhibition might reflect an important role in pre-hypertrophic differentiation. It is important to note, however, that the current study does not discriminate between direct and secondary effects of treatment.

Our results also demonstrate that *PPARγ* transcript levels in chondrocytes are regulated by GSK-3 activity, and thus link GSK-3 signalling and PPARγ. Inhibition of GSK-3 activity reduces *PPARγ* transcript levels suggesting that GSK-3 signalling is required for *PPARγ* expression. We have also shown that GSK-3β protein expression increases as chondrocytes hypertrophy (unpublished data). Whether this is a direct or indirect effect could not be answered in the current study. We further demonstrate reduced osteoblast-associated gene expression in response to GSK-3 inhibition. These observations contradict those reported by Kulkarni *et al*. [54], who described increased osteoblast-associated markers in murine mesenchymal cells following GSK-3 inhibition. These results may in part be explained by cell-type- or maturation-stage-specific effects. For example, one pathway affected by GSK-3β signalling, the Wnt/β-catenin pathway, has opposite effects on chondrogenic and osteogenic differentiation [55]; thus, inhibition of GSK-3β could cause opposing effects in these two lineages. Overexpression of GSK-3β in skeletal muscle is associated with increased adipose tissue mass [56]. Treatment of 3T3-L1 preadipocytes with GSK-3 inhibitors prevents differentiation, leading to the speculation that GSK-3β mediated adipogenesis might be involved in the development of obesity [57]. These results relate to those observed in the current study where GSK-3 inhibition reduces the lipid-storage effects of PPARγ activation in chondrocytes. Results from the current study therefore suggest that PPARγ-dependent lipid droplet size and number requires GSK-3 signalling. However, the role of GSK-3 in PPARγ signalling is complex as inhibitors of GSK-3 have been shown to improve insulin action and glucose metabolism in skeletal muscle [58, 59].

Although the role of PPARγ in chondrocytes remains incompletely resolved, the present study suggests that it is involved with lipid metabolism. This conclusion arises in part from the expression of PPARγ target genes *Lpl* and *Fabp4* in differentiating chondrocytes. The PPARγ target *Lpl* shows very similar expression patterns to *PPARγ2* in chondrocytes. Expression of both *Lpl* and *Fabp4* genes is enhanced by PPARγ agonists. Furthermore, chondrocytes were observed to possess more and enlarged lipid droplets in response to PPARγ stimulation as demonstrated by oil red O staining. These observations indicate active PPARγ proteins in differentiating chondrocytes. Although these observations have been partly described previously [60], this paper is the first to show that PPARγ-associated lipid metabolism in chondrocytes involves p38 MAPK and GSK-3 signalling. The current study thus shows that chondrocytes do indeed have the capacity to metabolize lipid. These may be significant findings in view of the increasing incidence of obesity. Understanding bone growth and factors regulating its expansion and linear growth are key issues in comprehending pathways leading to skeletal pathologies. Factors affecting bone growth may play vital roles in determining bone quality and predisposition to fractures and bone diseases in later life.

Acknowledgements

This work was supported by grants from the Canadian Institutes of Health Research. J.L. received a summer-studentship from the Institute for Musculoskeletal Health and Arthritis of the Canadian Institutes of Health Research. F.B holds the Canada Research Chair in Musculoskeletal Health.

References

1. **Tuan RS, Boland G, Tuli R.** Adult mesenchymal stem cells and cell-based tissue engineering. *Arthritis Res Ther.* 2003; 5: 32–45.
2. **de Crombrugghe B, Lefebvre V, Behringer RR, *et al.*** Transcriptional mechanisms of chondrocyte differentiation. *Matrix Biol.* 2000; 19: 389–94.
3. **Kronenberg HM.** PTHrP and skeletal development. *Ann NY Acad Sci.* 2006; 1068: 1–13.
4. **Lai LP, Mitchell J.** Indian hedgehog: its roles and regulation in endochondral bone development. *J Cell Biochem.* 2005; 96: 1163–73.
5. **Shimizu H, Yokoyama S, Asahara H.** Growth and differentiation of the developing limb bud from the perspective of chondrogenesis. *Dev Growth Differ.* 2007; 49: 449–54.
6. **Stanton LA, Beier F.** Inhibition of p38 MAPK signaling in chondrocyte cultures results in enhanced osteogenic differentiation of perichondral cells. *Exp Cell Res.* 2007; 313: 146–55.
7. **Tew SR, Hardingham TE.** Regulation of SOX9 mRNA in human articular chondrocytes involving p38 MAPK activation and mRNA stabilization. *J Biol Chem.* 2006; 281: 39471–9.
8. **Zhang R, Murakami S, Coustry F, *et al.*** Constitutive activation of MKK6 in chondrocytes of transgenic mice inhibits proliferation and delays endochondral bone formation. *Proc Natl Acad Sci USA.* 2006; 103: 365–70.
9. **Kapadia RM, Guntur AR, Reinhold MI, *et al.*** Glycogen synthase kinase 3 controls endochondral bone development: contribution of fibroblast growth factor 18. *Dev Biol.* 2005; 285: 496–507.
10. **Desvergne B, Wahli W.** Peroxisome proliferator-activated receptors: nuclear control of metabolism. *Endoc Rev.* 1999; 20: 649–88.
11. **Kota BP, Huang TH, Roufogalis BD.** An overview on biological mechanisms of PPARs. *Pharmacol Res.* 2005; 51: 85–94.
12. **Akune T, Ohba S, Kamekura S, *et al.*** PPARgamma insufficiency enhances osteogenesis through osteoblast formation from bone marrow progenitors. *J Clin Invest.* 2004; 113: 846–55.
13. **Berger JP, Akiyama TE, Meinke PT.** PPARs: therapeutic targets for metabolic disease. *Trends Pharmacol Sci.* 2005; 26: 244–51.
14. **Auboeuf D, Rieusset J, Fajas L, *et al.*** Tissue distribution and quantification of the expression of mRNAs of peroxisome proliferator-activated receptors and liver X receptor-alpha in humans: no alteration in adipose tissue of obese and NIDDM patients. *Diabetes.* 1997; 46: 1319–27.
15. **Braissant O, Foufelle F, Scotto C, *et al.*** Differential expression of peroxisome proliferator-activated receptors (PPARs): tissue distribution of PPAR-alpha, -beta, and -gamma in the adult rat. *Endocrinology.* 1996; 137: 354–66.
16. **Shao YY, Wang L, Hicks DG, *et al.*** Expression and activation of peroxisome proliferator-activated receptors in growth plate chondrocytes. *J Orthop Res.* 2005; 23: 1139–45.
17. **Evans RM, Barish GD, Wang YX.** PPARs and the complex journey to obesity. *Nat Med.* 2004; 10: 355–61.
18. **Wang YX, Zhang CL, Yu RT, *et al.*** Regulation of muscle fiber type and running endurance by PPARdelta. *PLoS Biology.* 2004; 2: 1532–9.
19. **Aperlo C, Pognonec P, Saladin R, *et al.*** cDNA cloning and characterization of the transcriptional activities of the hamster peroxisome proliferator-activated receptor haPPAR gamma. *Gene.* 1995; 162: 297–302.
20. **Dreyer C, Krey G, Keller H, *et al.*** Control of the peroxisomal beta-oxidation pathway by a novel family of nuclear hormone receptors. *Cell.* 1992; 68: 879–87.
21. **Fajas L, Auboeuf D, Raspé E, *et al.*** The organization, promoter analysis, and expression of the human PPARgamma gene. *J Biol Chem.* 1997; 272: 18779–89.
22. **Greene ME, Blumberg B, McBride OW, *et al.*** Isolation of the human peroxisome proliferator activated receptor gamma cDNA: expression in hematopoietic cells and chromosomal mapping. *Gene Expr.* 1995; 4: 281–99.
23. **Tontonoz P, Hu E, Graves RA, *et al.*** mPPAR gamma 2: tissue-specific regulator of an adipocyte enhancer. *Genes Dev.* 1994; 8: 1224–34.
24. **Zhu Y, Alvares K, Huang Q, *et al.*** Cloning of a new member of the peroxisome proliferator-activated receptor gene family from mouse liver. *J Biol Chem.* 1993; 268: 26817–20.
25. **Zhu Y, Qi C, Korenberg JR, *et al.*** Structural organization of mouse peroxisome proliferator-activated receptor gamma (mPPAR gamma) gene: alternative promoter use and different splicing yield two mPPAR gamma isoforms. *Proc Natl Acad Sci USA.* 1995; 92: 7921–5.
26. **Tontonoz P, Hu E, Spiegelman BM.** Stimulation of adipogenesis in fibroblasts by PPAR gamma 2, a lipid-activated transcription factor. *Cell* 1994; 79: 1147–56.
27. **Vidal-Puig AJ, Considine RV, Jimenez-Liñan M, *et al.*** Peroxisome proliferator-activated receptor gene expression in human tissues. Effects of obesity, weight loss, and regulation by insulin and glucocorticoids. *J Clin Invest.* 1997; 99: 2416–22.
28. **Michalik L, Desvergne B, Dreyer C, *et al.*** PPAR expression and function during vertebrate development. *Int J Dev Biol.* 2002; 46: 105–14.
29. **Brown JD, Plutzky J.** Peroxisome proliferator-activated receptors as transcriptional nodal points and therapeutic targets. *Circulation.* 2007; 115: 518–33.
30. **Heikkinen S, Auwerx J, Argmann CA.** PPARgamma in human and mouse physiology. *Biochim Biophys Acta.* 2007; 1771: 999–1013.
31. **Lehrke M, Lazar MA.** The many faces of PPARgamma. *Cell.* 2005; 123: 993–9.
32. **Bordji K, Grillasca JP, Gouze JN, *et al.*** Evidence for the presence of peroxisome proliferator-activated receptor (PPAR) alpha and gamma and retinoid Z receptor in cartilage. PPARgamma activation modulates the effects of interleukin-1beta on rat chondrocytes. *J Biol Chem.* 2000; 275: 12243–50.
33. **Wang L, Shao YY, Ballock RT.** Peroxisome proliferator activated receptor-gamma (PPARgamma) represses thyroid hormone signaling in growth plate chondrocytes. *Bone.* 2005; 37: 305–12.
34. **Poleni PE, Bianchi A, Etienne S, *et al.*** Agonists of peroxisome proliferators-activated receptors (PPAR) alpha, beta/delta or gamma reduce transforming growth factor (TGF)-beta-induced proteoglycans' production in chondrocytes. *Osteoarthritis Cartilage.* 2007; 15: 493–505.
35. **Afif H, Benderdour M, Mfuna-Endam L, *et al.*** Peroxisome proliferator-activated receptor gamma1 expression is diminished in human osteoarthritic cartilage and is downregulated by interleukin-1beta in articular chondrocytes. *Arthritis Res Ther.* 2007; 9: R31.

36. **Berger JP, Akiyama TE, Meinke PT.** PPARs: therapeutic targets for metabolic disease. *Trends Pharmacol Sci*. 2005; 26: 244–51.
37. **Kirkpatrick CJ, Mohr W, Haferkamp O.** Lipid storage in cultured articular chondrocytes due to prostanoid precursors and a prostanoid synthesis inhibitor. *Cell Tissue Res*. 1982; 224: 441–8.
38. **Stanton LA, Sabari S, Sampaio AV, *et al.*** p38 MAP kinase signaling is required for hypertrophic chondrocyte differentiation. *Biochem J*. 2004; 378: 53–62.
39. **Agoston H, Khan S, James CG, *et al.*** C-type natriuretic peptide regulates endochondral bone growth through p38 MAP kinase-dependent and -independent pathways. *BMC Dev Biol*. 2007; 7: 18.
40. **Stanton LA, Fenhalls G, Lucas A, *et al.*** Immunophenotyping of macrophages in human pulmonary tuberculosis and sarcoidosis. *Int J Exp Pathol*. 2003; 84: 289–304.
41. **Shao YY, Wang L, Hicks DG, *et al.*** Expression and activation of peroxisome proliferator-activated receptors in growth plate chondrocytes. *J Orthop Res*. 2005; 23: 1139–45.
42. **Wang L, Shao YY, Ballock RT.** Peroxisome proliferator activated receptor-gamma (PPARgamma) represses thyroid hormone signaling in growth plate chondrocytes. *Bone*. 2005; 37: 305–12.
43. **Li M, Pan LC, Simmons HA, *et al.*** Surface-specific effects of a PPARgamma agonist, darglitazone, on bone in mice. *Bone*. 2006; 39: 796–806.
44. **Lin TH, Yang RS, Tang CH, *et al.*** PPARgamma inhibits osteogenesis *via* the down-regulation of the expression of COX-2 and iNOS in rats. *Bone*. 2007; 41: 562–74.
45. **Zhou H, Yang X, Wang N, *et al.*** Tigogenin inhibits adipocytic differentiation and induces osteoblastic differentiation in mouse bone marrow stromal cells. *Mol Cell Endocrinol*. 2007; 270: 17–22.
46. **Schild RL, Sonnenberg-Hirche CM, Schaiff WT, *et al.*** The kinase p38 regulates peroxisome proliferator activated receptor-gamma in human trophoblasts. *Placenta*. 2006; 27: 191–9.
47. **Ricote M, Huang JT, Welch JS, *et al.*** The peroxisome proliferator-activated receptor(PPARgamma) as a regulator of monocyte/macrophage function. *J Leukoc Biol*. 1999; 66: 733–9.
48. **Pellieux C, Montessuit C, Papageorgiou I, *et al.*** Inactivation of peroxisome proliferator-activated receptor isoforms alpha, beta/delta, and gamma mediate distinct facets of hypertrophic transformation of adult cardiac myocytes. *Pflugers Arch*. 2007; 455: 443–54.
49. **Su W, Bush CR, Necela BM, *et al.*** Differential expression, distribution, and function of PPAR-gamma in the proximal and distal colon. *Physiol Genomics*. 2007; 30: 342–53.
50. **Chang F, Jaber LA, Berlie HD, *et al.*** Evolution of peroxisome proliferator-activated receptor agonists. *Ann Pharmacother*. 2007; 41: 973–83.
51. **Escher P, Wahli W.** Peroxisome proliferator-activated receptors: insight into multiple cellular functions. *Mutat Res*. 2000; 448: 121–38.
52. **Phornphutkul C, Wu KY, Gruppuso PA.** The role of insulin in chondrogenesis. *Mol Cell Endocrinol*. 2006; 249: 107–15.
53. **Aouadi M, Laurent K, Prot M, *et al.*** Inhibition of p38MAPK increases adipogenesis from embryonic to adult stages. *Diabetes*. 2006; 55: 281–9.
54. **Kulkarni NH, Onyia JE, Zeng Q, *et al.*** Orally bioavailable GSK-3alpha/beta dual inhibitor increases markers of cellular differentiation *in vitro* and bone mass *in vivo*. *J Bone Miner Res*. 2006; 21: 910–20.
55. **Day TF, Guo X, Garrett-Beal L, *et al.*** Wnt/beta-catenin signaling in mesenchymal progenitors controls osteoblast and chondrocyte differentiation during vertebrate skeletogenesis. *Dev Cell*. 2005; 8: 739–50.
56. **Pearce NJ, Arch JR, Clapham JC, *et al.*** Development of glucose intolerance in male transgenic mice overexpressing human glycogen synthase kinase-3beta on a muscle-specific promoter. *Metabolism*. 2004; 53: 1322–30.
57. **Ross SE, Hemati N, Longo KA, *et al.*** Inhibition of adipogenesis by Wnt signaling. *Science*. 2000; 289: 950–3.
58. **Dokken BB, Sloniger JA, Henriksen EJ.** Acute selective glycogen synthase kinase-3 inhibition enhances insulin signaling in prediabetic insulin-resistant rat skeletal muscle. *Am J Physiol Endocrinol Metab*. 2005; 288: E1188–94.
59. **Nikoulina SE, Ciaraldi TP, Mudaliar S, *et al.*** Inhibition of glycogen synthase kinase 3 improves insulin action and glucose metabolism in human skeletal muscle. *Diabetes*. 2002; 51: 2190–8.
60. **Wang L, Shao YY, Ballock RT.** Peroxisome proliferator-activated receptor-gamma promotes adipogenic changes in growth plate chondrocytes *in vitro*. *PPAR Res*. 2006; 2006: 1–8.